



**HAL**  
open science

## **Otx2 controls neuron subtype identity in ventral tegmental area and antagonizes vulnerability to MPTP**

Antonio Simeone, Michela Di Salvio, Luca Giovanni Di Giovannantonio, Dario Acampora, Raffaele Prosperi, Daniela Omodei, Nilima Prakash, Wolfgang Georg Wurst

### ► To cite this version:

Antonio Simeone, Michela Di Salvio, Luca Giovanni Di Giovannantonio, Dario Acampora, Raffaele Prosperi, et al.. Otx2 controls neuron subtype identity in ventral tegmental area and antagonizes vulnerability to MPTP. *Nature Neuroscience*, 2010, 10.1038/nn.2661 . hal-00591155

**HAL Id: hal-00591155**

**<https://hal.science/hal-00591155>**

Submitted on 7 May 2011

**HAL** is a multi-disciplinary open access archive for the deposit and dissemination of scientific research documents, whether they are published or not. The documents may come from teaching and research institutions in France or abroad, or from public or private research centers.

L'archive ouverte pluridisciplinaire **HAL**, est destinée au dépôt et à la diffusion de documents scientifiques de niveau recherche, publiés ou non, émanant des établissements d'enseignement et de recherche français ou étrangers, des laboratoires publics ou privés.

**Otx2 controls neuron subtype identity in ventral tegmental area and antagonizes vulnerability to MPTP**

Michela Di Salvio<sup>1,5</sup>, Luca Giovanni Di Giovannantonio<sup>1,5</sup>, Dario Acampora<sup>1,2</sup>, Raffaele Proserpi<sup>3</sup>, Daniela Omodei<sup>1</sup>, Nilima Prakash<sup>4</sup>, Wolfgang Wurst<sup>4</sup> and Antonio Simeone<sup>1,2,6</sup>

<sup>1</sup>CEINGE Biotechnologie Avanzate, via Comunale Margherita 482, 80145 Naples, Italy and SEMM European School of Molecular Medicine - Naples site, Italy; <sup>2</sup>Institute of Genetics and Biophysics “A. Buzzati-Traverso”, CNR, Via P. Castellino 111, 80131 Naples, Italy; <sup>3</sup>Dipartimento di Matematica e Statistica, Università degli Studi del Sannio, Via delle Puglie 82, 82100 Benevento, Italy; <sup>4</sup>Helmholtz Zentrum München, Technische Universität München, Deutsches Zentrum für Neurodegenerative Erkrankungen München, Institute of Developmental Genetics, 85764 Munich/Neuherberg, Max-Planck-Institute of Psychiatry, Molecular Neurogenetics, Kraepelinstr. 2-16, 80804 Munich, Germany

<sup>5</sup>These authors equally contributed to the work

<sup>6</sup>**Corresponding author:** [simeone@ceinge.unina.it](mailto:simeone@ceinge.unina.it); Tel. +39 081 37 37 868

**Total words:** 3462 (Introduction, Results and Discussion)

**ABSTRACT**

Mesencephalic-diencephalic Dopaminergic neurons control locomotor activity and emotion and are affected in neurodegenerative and psychiatric diseases. The homeoprotein Otx2 is restricted to ventral tegmental area (VTA) neurons prevalently complementary to those expressing *Girk2* and glycosylated active form of Dopamine transporter (*Dat*). High level of glycosylated-*Dat* identifies neurons with efficient Dopamine uptake and pronounced vulnerability to Parkinsonian degeneration. We found that Otx2 controls neuron subtype identity by antagonizing molecular and functional features of dorsal-lateral VTA such as *Girk2* and *Dat* expression. Through this control, Otx2 limits the number of VTA neurons with efficient Dopamine uptake and confers resistance to the MPTP neurotoxin. Ectopic Otx2 expression also provides neurons of the Substantia Nigra with efficient neuroprotection to MPTP. These findings show that Otx2 is required to specify neuron subtype identity in VTA and may antagonize vulnerability to the Parkinsonian toxin MPTP.

## INTRODUCTION

Mesencephalic and diencephalic dopaminergic (mdDA) progenitors give rise to two major subgroups corresponding to the A9 neurons of the substantia nigra pars compacta (SNpc) and the A10 neurons of the ventral tegmental area (VTA)<sup>1-5</sup>. SNpc neurons originate from both anterior prosomeres and mesencephalon while VTA neurons from mesencephalic dopaminergic (mesDA) progenitors<sup>5,6,7</sup>. MdDA neurons play a crucial role in the control of motor, sensorimotor and motivated behaviours<sup>8</sup>. Degeneration of SNpc neurons is associated to the characteristic symptoms of Parkinson's disease (PD) while abnormal functioning of VTA neurons is involved in psychiatric disorders. Relevant advances have been made in the comprehension of the molecular mechanism controlling neurogenesis and survival of mdDA neurons<sup>4,6,9-29</sup>. Nevertheless, little is known about the molecular basis determining phenotypic and functional diversity between and within SNpc and VTA neurons. For example, Dopamine (DA) uptake may be differentially regulated in SNpc and VTA neurons by the cellular level of the glycosylated active form of the Dopamine transporter (glyco-Dat), whose distribution is not uniform, but preferentially restricted to SNpc and dorsal-lateral VTA neurons<sup>30</sup>, which are also more sensitive to neurodegeneration caused by PD or 1-methyl-4-phenyl-1,2,3,6-tetrahydropyridine-HCl (MPTP) toxin<sup>30-33</sup>. Furthermore, the fact that several gene markers are expressed in specific subsets of VTA and SNpc neurons reinforces the idea that these two groups of neurons may include multiple subtypes, potentially determining a complex source of functional diversity<sup>34,35</sup>. In this context, Calbindin D28K (Calb) is prevalently expressed in a relevant fraction of VTA neurons, while the G-protein-gated inwardly rectifying K<sup>+</sup> channel (Girk2) and the aldehyde dehydrogenase family 1, subfamily A1 gene also known as Ahd2 or Aldh1A1 are both expressed in a relevant proportion of SNpc neurons and in a subset of VTA neurons<sup>4,7,36-40</sup>. Very little is known about genetic function(s) controlling specification and/or

maintenance of these neuronal subpopulations. We have previously concentrated our efforts on the role exerted by the transcription factor Otx2 in mdDA neurogenesis<sup>6,27-29</sup>. Recently, we and others discovered that in adult mice Otx2 is expressed in a relevant subset of VTA neurons and excluded from those of the SNpc<sup>34,38</sup>. In VTA neurons Otx2 is prevalently co-expressed with Calb and Ahd2 and only marginally with Girk2 which, in turn is confined to dorsal-lateral VTA neurons co-expressing high level of glyco-Dat<sup>30,38</sup>. Here, through the study of loss and gain of function mouse models, we investigated whether Otx2 is required for providing VTA neurons with specific identity and functional features. We show that Otx2 is required in the VTA to specify neuronal subtype identity, and may be involved in the regulation of DA metabolism by restricting efficient DA uptake to the Otx2<sup>+</sup> neurons of SNpc and dorsal-lateral VTA.

## RESULTS

### Mouse models to study Otx2 in adult mdDA neurons

The role of Otx2 in adult mdDA neurons was investigated by analyzing the phenotype of mice lacking Otx2 in the VTA and that of mice activating increasing dosages of Otx2 in the SNpc and VTA. To this aim we employed a Cre mouse model in which the Ires-Cre recombinase (ICre) was inserted into the 3' untranslated region of the Dopamine transporter gene (*Dat*<sup>ICre/+</sup>)<sup>41</sup> without affecting Dat synthesis. To investigate selectively Otx2<sup>+</sup> neurons in the VTA even in the absence of the Otx2 protein, the *Otx2*<sup>fllox</sup> allele was coupled with the *Otx2*<sup>GFP</sup> allele<sup>38,42</sup> by generating *Dat*<sup>ICre/+</sup>; *Otx2*<sup>GFP/+</sup> control and *Dat*<sup>ICre/+</sup>; *Otx2*<sup>GFP/fllox</sup> mutant mice. The Cre efficiency was analyzed in *Dat*<sup>ICre/+</sup>; *Otx2*<sup>GFP/fllox</sup>; *R26R-LacZ* and *Dat*<sup>ICre/+</sup>; *Otx2*<sup>GFP/+</sup>; *R26R-LacZ* triple mutants at postnatal day 10 (P10) (**Fig. 1a-f**) by monitoring the combined expression of Otx2, GFP, TH and βGal. We found that, as revealed by the βGal activation in all mdDA TH<sup>+</sup> neurons of control and mutant mice (**Fig. 1e,f**) and the lack of Otx2 immunoreactivity in TH<sup>+</sup> neurons of mutant brains (**Fig. 1a,b**), the efficiency of the Cre activity was high and specific. Indeed, the residual Otx2<sup>+</sup>-GFP<sup>+</sup> neurons were TH<sup>-</sup> (compare **Fig. 1a,c** to **b,d**), confirming that about 20% of the Otx2<sup>+</sup> neurons were not DA neurons<sup>38</sup>. In parallel, the *Dat*<sup>ICre/+</sup> model was also used to generate an allelic series of conditional mutants over-expressing Otx2 with an increasing dosage. To this aim we employed the *tOtx2*<sup>ov/+</sup> transgenic mouse model<sup>6</sup> and a new mutant carrying an Otx2 conditionally activable allele in the *Rosa26* (*R26*) locus (*R26*<sup>Otx2/+</sup>) (**Supplementary Fig. 1** and Methods). To assess the functionality of the *R26*<sup>Otx2</sup> allele and the relative level of Otx2 protein, we targeted the CreER-recombinase in the second *R26* allele of the *R26*<sup>Otx2/+</sup> ES cell clone. The level of the Otx2 protein was assayed by western blot 24 hours after 4-hydroxytamoxifen (tamoxifen) administration and compared to untreated *R26*<sup>Otx2/CreER</sup> ES

cells and to tamoxifen-treated  $R26^{CreER/+};tOtx2^{ov/+}$  ES cells<sup>6</sup>. As deduced by densitometric analysis, the Otx2 level in  $R26^{Otx2/CreER}$  ES cells was about 1.5 and 3 fold higher than that detected in tamoxifen treated  $R26^{CreER/+};tOtx2^{ov/+}$  and untreated  $R26^{Otx2/CreER}$  ES cells, respectively (**Supplementary Fig. 1c**). The activation of Otx2 in mdDA neurons was analyzed in E18.5 and adult  $Dat^{ICre/+};tOtx2^{ov/+}$ ,  $Dat^{ICre/+};R26^{Otx2/+}$ ,  $Dat^{ICre/+};tOtx2^{ov/ov}$ ,  $Dat^{ICre/+};R26^{Otx2/Otx2}$  and  $Dat^{ICre/+};tOtx2^{ov/ov};R26^{Otx2/Otx2}$  mutants (**Fig. 1g-l** and data not shown). In all these mutants, Otx2 activation was ubiquitously detected in mdDA neurons with an increasing intensity paralleling the number of activated Otx2 extra-copies (**Fig. 1g-l** and data not shown). In particular, the Otx2 staining detected in  $Dat^{ICre/+};R26^{Otx2/Otx2}$  and  $Dat^{ICre/+};R26^{Otx2/Otx2};tOtx2^{ov/ov}$  mutants mirrored quite well the staining of the endogenous Otx2 in VTA (compare **Fig. 1j** to **h,i**). All these mutants were healthy, fertile and apparently normal.

### Otx2 in adult mdDA neurons

We previously reported that in the VTA the majority of the Otx2<sup>+</sup>-TH<sup>+</sup> neurons co-expressed Calb and/or Ahd2 and only a small fraction of them Girk2<sup>38</sup>. Therefore, we first analyzed in  $Dat^{ICre/+};Otx2^{GFP/+}$  control and  $Dat^{ICre/+};Otx2^{GFP/flox}$  mutant brains ( $n = 10$ /genotype) whether the lack of Otx2 affected the survival of TH<sup>+</sup>-Otx2<sup>+</sup> VTA neurons by determining the percentage of GFP<sup>+</sup> neurons co-expressing or not TH. No relevant difference between control and mutant mice was detected in the number of GFP<sup>-</sup>-TH<sup>+</sup>, GFP<sup>+</sup>-TH<sup>+</sup> and GFP<sup>+</sup>-TH<sup>-</sup> neurons (**Fig. 2a** and **Supplementary Table 1**). Then, we investigated whether in the absence of Otx2, the identity of GFP<sup>+</sup> neurons was altered by determining the percentage of GFP<sup>+</sup> neurons co-expressing Calb, Ahd2 or Girk2. A similar percentage of GFP<sup>+</sup>-Calb<sup>+</sup> and GFP<sup>+</sup>-Ahd2<sup>+</sup> neuronal subsets was detected in control and mutant mice (**Fig. 2b,g-j**), while the percentage of GFP<sup>+</sup>-Girk2<sup>+</sup> neurons resulted remarkably increased in mice lacking Otx2 (\*\* $P << 0.001$ )

(**Fig. 2b,k–n** and **Supplementary Table 1**). This increase was particularly evident in the central VTA (arrows in **Fig. 2m,n**). Then, we analyzed in mutants lacking *Otx2*, the expression of *Pitx3*, *Foxa2* and *Nurr1*, which play crucial roles in the establishment and survival of mdDA neurons<sup>4,25,43</sup>, and no evident abnormalities were detected in the expression of these genes (**Supplementary Fig. 2a–f**). These findings indicate that *Otx2* is not required for survival of VTA neurons and expression of *Calb*, *Ahd2*, *Pitx3*, *Nurr1* or *Foxa2* while it is required to antagonize prevalently in neurons of the central VTA the expression of *Girk2*, a marker of the dorsal-lateral VTA. Then, we investigated whether ectopic expression of *Otx2* in  $TH^+Otx2^-$  neurons of SNpc and VTA and over-expression in  $TH^+Otx2^+$  VTA neurons may affect survival and/or identity of these neurons. In all the genetic combinations analyzed ( $n = 10$ ), the number of SNpc and VTA neurons was very similar to that of *Dat*<sup>ICre/+</sup> control mice ( $P \geq 0.22$  for SNpc;  $P \geq 0.24$  in VTA) (**Supplementary Fig. 3** and **Supplementary Table 1**). Analysis of  $TH^+$  subpopulations expressing *Calb* or *Ahd2* or *Girk2* revealed no significant difference in the SNpc of *Dat*<sup>ICre/+</sup>;*R26*<sup>Otx2/Otx2</sup> ( $n = 7$ ) and *Dat*<sup>ICre/+</sup>;*R26*<sup>Otx2/Otx2</sup>;*tOtx2*<sup>ov/ov</sup> ( $n = 7$ ) mice ( $P \geq 0.1$  for *Calb*;  $P \geq 0.18$  for *Ahd2*;  $P \geq 0.12$  for *Girk2*) (**Supplementary Fig. 4**), while in the VTA of these mutants a significant reduction in the percentage of *Girk2*<sup>+</sup>- $TH^+$  neurons was observed ( $*P \ll 0.001$ ;  $**P \ll 0.001$ ) (**Fig. 3a,h–j** and **Supplementary Table 1**). Noteworthy, in the lateral-dorsal corner of the VTA, where *Girk2*<sup>+</sup> neurons were normally confined, few of them were detected in *Otx2* mutant mice (arrows in **Fig. 3h–j**). Finally, we monitored the expression of *Pitx3*, *Foxa2* and *Nurr1* and, as previously shown for mutants lacking *Otx2*, none of these genes exhibited an altered expression (**Supplementary Fig. 2g–r**). These findings support previous results on mice lacking *Otx2* and indicate that even at high dosage, *Otx2* is apparently unable to affect identity and/or survival of SNpc neurons. Moreover, the fact that in *Dat*<sup>ICre</sup>;*R26*<sup>Otx2/+</sup> and *Dat*<sup>ICre/+</sup>;*tOtx2*<sup>ov/ov</sup> mice, which activated a lower level of *Otx2*, no substantial abnormalities

were observed (data not shown), suggests that in the VTA Otx2 may alter the expression of Girk2 only at a level similar to that of the endogenous gene.

### **Otx2 confines high glyco-Dat to dorsal-lateral VTA neurons**

Proper DA uptake represents a crucial step for DA signalling. This event is controlled by the distribution and membrane concentration of the glycosylated form of Dat<sup>30</sup>, whose expression at high level is detected in the somata of nigrostriatal SNpc neurons and excluded from the majority of mesolimbic VTA neurons<sup>30,44,45</sup>. Based on this, we first investigated Otx2 and glyco-Dat expression in wild-type mice by using a glyco-Dat antibody<sup>30</sup>. We found that in the VTA the expression of Otx2 and glyco-Dat was largely complementary (**Fig. 4a,b**), thus indicating that Otx2 is prevalently expressed in neurons with a reduced DA uptake. In addition, glyco-Dat co-localized with Girk2 expression (**Fig. 4c,d**). Therefore, we analyzed whether loss or ectopic expression of Otx2 may influence level and distribution of glyco-Dat. We found that the percentage of GFP<sup>+</sup>-glyco-Dat<sup>+</sup> neurons was significantly higher in *Dat*<sup>ICre/+</sup>;*Otx2*<sup>GFP/flox</sup> mutants (24% vs 15% of control mice \**P* <<0.001) (**Fig. 4e-i** and **Supplementary Table 1**) and, as for Girk2, the number of GFP<sup>+</sup>-glyco-Dat<sup>+</sup> neurons was increased prevalently in the central VTA (arrows in **Fig. 4h**). Consistent with this, the striatal amount of glyco-Dat and the percentage of SNpc and VTA TH<sup>+</sup> neurons expressing high level of glyco-Dat was remarkably diminished in *Dat*<sup>ICre/+</sup>;*R26*<sup>Otx2/Otx2</sup> (data not shown) and *Dat*<sup>ICre/+</sup>;*R26*<sup>Otx2/Otx2</sup>;*tOtx2*<sup>ov/ov</sup> mutants (16% vs 49.4% of control mice \**P* <<0.001 for the SNpc, and 9% vs 24.6 of control mice \*\**P* <<0.001 for the VTA) (**Fig. 4j-s** and **Supplementary Table 1**). The same analysis performed with a second antibody against glyco-Dat showed very similar results (**Supplementary Fig. 5** and **Supplementary Table 2**). These data suggest that Otx2 is required to confine VTA neurons expressing high level of glyco-Dat to the dorsal-lateral VTA, and, through this antagonism, by limiting the number of

VTA neurons with efficient DA uptake, Otx2 may modulate DA signalling in neurons of the central VTA.

### **Otx2 negatively controls *Dat* mRNA expression**

To investigate the mechanism by which Otx2 controls the level of glyco-Dat, we analyzed *Dat* level in cell-extracts of ventral pretectum and mesencephalon with a third antibody recognizing also the non-glycosylated form of *Dat* (non-glyco-Dat). In *Dat*<sup>ICre/+</sup>;*R26*<sup>Otx2/Otx2</sup>;*tOtx2*<sup>ov/ov</sup> mutants, glyco-Dat and non-glyco-Dat protein levels appeared both proportionally decreased (**Fig. 5a**), suggesting that the diminished level of glyco-Dat should not reflect an impairment in the glycosylation process. Then, we analyzed by semi-quantitative RT-PCR the *Dat* mRNA level. A significant reduction was detected for *Dat* mRNA in *Dat*<sup>ICre/+</sup>;*R26*<sup>Otx2/Otx2</sup>;*tOtx2*<sup>ov/ov</sup> mutants (about 65% by densitometric scanning), while virtually no difference between mutants and control mice was observed for *TH* and *Nurr1* (compare in **Fig. 5b** lanes 1 and 2 to 3 and 4, respectively). To strengthen these findings, we performed in situ hybridization experiments and compared the distribution and amount of *Dat* mRNA to those of glyco-Dat. We found that, compared to control brain, the number of neurons expressing high level of *Dat* mRNA and glyco-Dat was increased in the central VTA of *Dat*<sup>ICre/+</sup>;*Otx2*<sup>GFP/flox</sup> mice (**Fig. 5c–f**), while, in *Dat*<sup>ICre/+</sup>;*R26*<sup>Otx2/Otx2</sup>;*tOtx2*<sup>ov/ov</sup> mutants the number of this neurons was heavily diminished in both SNpc and VTA (**Fig. 5g–n**). Together these findings suggest that reduced synthesis of glyco-Dat is primarily caused by an Otx2-mediated negative control of *Dat* mRNA level. This control however maybe direct or indirect.

### **Otx2 controls SNpc and VTA differential MPTP sensitivity**

Glyco-Dat efficiently binds the DA analogue neurotoxin MPTP<sup>30,31,46,47</sup>. Therefore, we studied whether *Otx2* depletion in the VTA or its ectopic expression in SNpc and in all the VTA neurons may alter the vulnerability of these neurons to MPTP-induced neurodegeneration. To this aim, we compared cell numbers and ratio between MPTP-treated ( $n = 10/\text{genotype}$ ) and untreated ( $n = 10/\text{genotype}$ ) neurons in 14-16 week old control and mutant brains (**Fig. 6** and **Supplementary Table 3**). First we determined the number of TH<sup>+</sup>, GFP<sup>+</sup>-TH<sup>+</sup> and GFP<sup>-</sup>-TH<sup>+</sup> neurons in the VTA of MPTP-treated (100 mg/Kg) and untreated *Dat*<sup>ICre/+</sup>;*Otx2*<sup>GFP/+</sup> control and *Dat*<sup>ICre/+</sup>;*Otx2*<sup>GFP/flox</sup> mutant mice. In this context, GFP<sup>-</sup>-TH<sup>+</sup> neurons represented a sort of internal control, since, in principle, they should not be additionally affected by the lack of *Otx2*. We found that, while in MPTP-untreated mice the number of TH<sup>+</sup>, GFP<sup>+</sup>-TH<sup>+</sup> and GFP<sup>-</sup>-TH<sup>+</sup> neurons was very similar in controls and mutants (**Fig. 2a** and **Supplementary Table 3**), in MPTP-treated mice a significant reduction in the number of total TH<sup>+</sup> neurons ( $*P < 0.001$ ) and GFP<sup>+</sup>-TH<sup>+</sup> neurons ( $**P 0.005$ ) was detected in *Dat*<sup>ICre/+</sup>;*Otx2*<sup>GFP/flox</sup> mutant mice (**Fig. 6a** and **Supplementary Table 3**). Importantly, the GFP<sup>-</sup>-TH<sup>+</sup> neuronal subset was not significantly affected by the MPTP treatment ( $***P 0.4$ ) (**Fig. 6a** and **Supplementary Table 3**). Then, we determined the ratio (in %) between MPTP-treated and untreated neuronal subpopulations in control and mutant mice. In control mice, MPTP treatment resulted in a 15% reduction of total TH<sup>+</sup> neurons (**Fig. 6c**); sorting of TH<sup>+</sup> neurons in those expressing *Otx2* (GFP<sup>+</sup>-TH<sup>+</sup>) or not (GFP<sup>-</sup>-TH<sup>+</sup>) revealed that the vulnerability to MPTP was much higher for the GFP<sup>-</sup>-TH<sup>+</sup> neuronal subset (24% reduction of GFP<sup>-</sup>-TH<sup>+</sup> subset vs 8% reduction of the GFP<sup>+</sup>-TH<sup>+</sup> subset) (**Fig. 6c**), and similar to that observed for SNpc neurons in wild-type (data not shown) or *Dat*<sup>ICre/+</sup> control mice (**Fig. 6f**). Compared to control mice, in *Dat*<sup>ICre/+</sup>;*Otx2*<sup>GFP/flox</sup> mutants, the ratio between MPTP-treated and untreated total TH<sup>+</sup> neurons was diminished by about 8% ( $*P 0.001$ ) (**Fig. 6c** and **Supplementary Table 3**), but this reduction was almost completely due to loss of GFP<sup>+</sup>-TH<sup>+</sup>

neurons (78% vs 92% of control mice;  $**P \ll 0.001$ ) (**Fig. 6c**). No significant difference was observed for the GFP<sup>-</sup>-TH<sup>+</sup> subpopulation in control and mutant mice (73% vs 76% of control mice;  $***P 0.1$ ) (**Fig. 6c**). Then, we studied whether the neuroprotection was effective also at a higher amount of MPTP (125 mg/Kg) (**Fig. 6b,d**). Compared to control mice ( $n = 8$ ),  $Dat^{ICre/+};Otx2^{GFP/flox}$  ( $n = 8$ ) mutants exhibited a 12% and 17% reduction of total TH<sup>+</sup> (70% vs 82% of control mice,  $*P \ll 0.001$ ) and GFP<sup>+</sup>-TH<sup>+</sup> (73% vs 90% of control mice  $**P \ll 0.001$ ) neurons. No significant difference was observed for the GFP<sup>-</sup>-TH<sup>+</sup> subset (66% vs 63% of control embryos  $***P 0.15$ ) (**Fig. 6b,d** and **Supplementary Table 3**). Noteworthy, also in this experiment the vulnerability of VTA neurons lacking Otx2 was similar to that of SNpc neurons  $Dat^{ICre/+};Otx2^{GFP/+}$  mice (**Fig. 6d** and **Supplementary Table 3**). These findings indicate that *i*) Otx2 may selectively provide Otx2<sup>+</sup> (GFP<sup>+</sup>)-TH<sup>+</sup> VTA neurons with reduced vulnerability to MPTP; *ii*) the Otx2<sup>-</sup> (GFP<sup>-</sup>)-TH<sup>+</sup> VTA subpopulation, which is prevalently composed by Girk2<sup>+</sup> neurons expressing high level of glyco-Dat, exhibits a sensitivity to MPTP similar to that of SNpc neurons; and *iii*) in the absence of Otx2 the vulnerability of VTA neurons is similar to that of the SNpc. Then, we investigated whether ubiquitous activation of Otx2 was able to provide SNpc and VTA neurons with resistance to MPTP. To this purpose, untreated and MPTP-treated (100 mg/Kg) 14-16 week old  $Dat^{ICre}$  ( $n = 10$ ) control mice were compared to  $Dat^{ICre};R26^{Otx2/Otx2}$  ( $n = 10$ ),  $Dat^{ICre};R26^{Otx2/Otx2};tOtx2^{ov/ov}$  ( $n = 10$ ) and  $Dat^{ICre/+};R26^{Otx2/+}$  ( $n = 10$ ) mutants. We found that, compared to  $Dat^{ICre/+}$  control mice, the number of total TH<sup>+</sup> neurons detected in  $Dat^{ICre/+};R26^{Otx2/Otx2}$  and  $Dat^{ICre/+};R26^{Otx2/Otx2};tOtx2^{ov/ov}$  mutants after MPTP treatment was remarkably higher in both SNpc ( $*P$  and  $**P \ll 0.001$ ) and VTA ( $*P < 0.001$  and  $**P \ll 0.001$ ) (**Fig. 6e** and **Supplementary Table 3**). The ratio (in %) between MPTP-treated and untreated neurons in SNpc and VTA confirmed that Otx2 activation in  $Dat^{ICre/+};R26^{Otx2/Otx2};tOtx2^{ov/ov}$  and  $Dat^{ICre/+};R26^{Otx2/Otx2}$  mice efficiently protected SNpc ( $*P$  and  $**P < 0.001$ ) and VTA ( $*P 0.0018$

and  $**P \ll 0.001$ ) neurons from MPTP neurotoxicity (**Fig. 6f**). In particular  $Dat^{ICre/+};R26^{Otx2/Otx2};tOtx2^{ov/ov}$  mice appeared almost completely insensitive to MPTP. Conversely, in  $Dat^{ICre/+};R26^{Otx2/+}$  mice a quite modest neuroprotection was detected (data not shown), thus suggesting that the Otx2 neuroprotective effect is dose-dependent and may be conferred to SNpc neurons and to the Otx2<sup>-</sup> VTA neuronal fraction. On the whole, this analysis suggests that Otx2 may remarkably contribute to the SNpc and VTA differential vulnerability to MPTP.

## DISCUSSION

Previous studies have indicated that Otx2 plays a crucial role in mesDA neurogenesis while it is apparently not required for differentiation of mdDA neurons of more anterior pretectal origin<sup>6,27-29</sup>. Recently, we have shown that in adult brains Otx2 expression is excluded from SNpc and restricted to neurons of the central and medial-ventral VTA, where it is co-expressed with Calb and/or Ahd2 and complementary to the majority of those expressing Girk2<sup>38</sup>. This restricted expression has led us to investigate whether Otx2 is required to control molecular identity and functional features of adult VTA neurons. Lack of Otx2 induces in neurons of the central VTA the expression of Girk2, which is prevalently confined to neurons of the dorsal-lateral VTA (**Supplementary Fig. 7**). Consistent with this, robust activation of Otx2 also in the Otx2<sup>-</sup> fraction of VTA neurons generates a relevant reduction in the number of Girk2<sup>+</sup> neurons (**Supplementary Fig. 7**). This suggests that Otx2 is cell-autonomously required in neurons of the central VTA to antagonize identity features of the dorsal-lateral VTA. Noteworthy, a major role for Otx2 in embryogenesis is to define the border between adjacent territories or compartments as in the case of the midbrain-hindbrain border or between progenitors of the mesDA and red nucleus compartments<sup>27,28</sup>. In these processes, Otx2 operates as a repressing factor by interacting with co-repressing molecules such as Grg4<sup>27,28,48</sup>. Based on this, our data are not in contrast with the possibility that VTA neurons are distributed in compartment-like subregions whose identity is maintained by a molecular code of transcription factors together with positive and negative interacting cofactors. In this context, Otx2 may represent one of these factors whose competence appeared limited to define the identity of central VTA and/or presumptive border between central and dorsal-lateral VTA. Then, we investigated whether Otx2 may also be involved in controlling relevant aspects determining the functioning of VTA neurons. To this aim we analyzed the distribution of glyco-Dat, which is required for the uptake of both DA and DA analogue toxin

MPTP<sup>30,31</sup>. Interestingly, as for *Girk2*, *Otx2* showed an extensive complementary expression also with glyco-Dat, and in mutants, lack of *Otx2* resulted in an increase of GFP<sup>+</sup>-glyco-Dat<sup>+</sup> neurons, while activation of *Otx2* generated a reduction of glyco-Dat<sup>+</sup> neurons (**Supplementary Fig. 7**). This suggests that *Otx2* may have a relevant role on DA signalling by suppressing excessive DA uptake in *Otx2*<sup>+</sup> neurons of the central VTA and confining those with efficient DA uptake to the dorsal-lateral VTA (**Supplementary Fig. 7**). Through this control, *Otx2* might likely contribute to define the VTA map of DA uptake. At the molecular level, our data indicate that *Otx2* modulates glyco-Dat levels by controlling negatively (directly or indirectly) the level of *Dat* mRNA rather than the glycosylation process. In this context, an attracting possibility is that in the central VTA *Otx2* might control *Dat* expression in antagonism with *Nurr1*, which is required for *Dat* expression<sup>12,25,49</sup>. A relevant consequence of *Otx2* ablation in the VTA is an increased vulnerability to the MPTP toxin likely due to a higher level of glyco-Dat and consequent increase of MPTP internalization<sup>30,31</sup>. Consistent with this, mice lacking *Otx2* and exposed to MPTP treatment show a significant and specific loss of GFP<sup>+</sup>-TH<sup>+</sup> neurons, which in control mice exhibit high resistance to MPTP toxicity. In contrast, the *Otx2*<sup>-</sup> population of VTA neurons shows in control and mutant mice a similar and more pronounced sensitivity to MPTP. These findings suggest that also the vulnerability to MPTP converges towards the existence of at least two major functionally distinct subpopulations of VTA neurons. The molecular basis controlling SNpc and VTA differential vulnerability to MPTP and Parkinsonian neurodegeneration represents a yet unsolved key issue. Interestingly, the MPTP vulnerability exhibited by VTA neurons of mice lacking *Otx2* is comparable to that of normal SNpc neurons, and robust ectopic expression of *Otx2* in SNpc generates high resistance of these neurons to MPTP. These findings suggest that *Otx2* is responsible, at least in part, for SNpc and VTA differential vulnerability to MPTP-induced neurodegeneration. Noteworthy, except for *Dat* expression, no

abnormality was detected for *Girk2*, *Ahd2*, *Calb*, *Pitx3*, *Foxa2* and *Nurr1* expression in the SNpc of mutants activating *Otx2*, suggesting that factors other than *Otx2* may be required for SNpc neuronal identity. This is similar to findings previously reported for mdDA progenitors in pretectum and mesencephalon, both expressing *Otx2* but with only those belonging to the mesencephalon responding to gain or loss of *Otx2*<sup>6</sup>.

**ACKNOWLEDGMENTS**

The authors would like to thank D. Grieco and T. Russo for helpful discussions and criticisms on the manuscript; S. Casola for the *R26* targeting vector; G. Corte for the *Otx2* antibody; and the staff of the CEINGE animal house for excellent animal care. We are grateful to E. Bricola for typing the manuscript. This work was supported by the FP7 for the project mdDA NEURODEV (222999) to A.S. and W.W.; the FP6 project for the EUTRACC Integrated Project (LSHG-CT-2007-037445) to A.S. and W.W.; the “Stem Cell Project” of Fondazione Roma and the Italian Association for Cancer Research (AIRC) to A.S.; and the Federal Ministry of Education and Research (BMBF) in the framework of the National Genome Research Network (NGFN+ Functional Genomics of Parkinson Disease FKZ 01GS08174) to W.W.

**AUTHOR CONTRIBUTION**

M.D.S. and L.G.D. performed the experiments; D.A. generated the *Otx2* mutant mice; R.P. performed the statistical analysis; D.O. and N.P. contributed to the phenotypic analysis; W.W. contributed to the interpretation of results and the writing of the manuscript; A.S. designed and interpreted the experiments and wrote the manuscript.

**AUTHOR DECLARATION**

The authors declare no competing financial interests.

**FIGURE LEGENDS**

**Fig. 1.** Otx2 post-mitotic inactivation and over-expression. **(a–f)** Immunohistochemistry experiments on P10  $Dat^{ICre};Otx2^{GFP/+};R26R-LacZ$  and  $Dat^{ICre};Otx2^{GFP/flox};R26R-LacZ$  mice with Otx2-TH **(a,b)**, Otx2-GFP **(c,d)** and  $\beta$ Gal-TH **(e,f)** show that Otx2 is inactivated in TH<sup>+</sup> neurons **(a,b)**, the residual Otx2<sup>+</sup>-GFP<sup>+</sup> neurons are TH<sup>-</sup> **(b,d)**, and  $\beta$ Gal from the *R26* locus is ubiquitously activated in TH<sup>+</sup> neurons by *Dat*-driven ICre recombinase **(e,f)**. **(g–l)** Otx2-TH immunostaining of E18.5  $Dat^{ICre/+}$  **(g,j)**,  $Dat^{ICre/+};R26^{Otx2/Otx2}$  **(h,k)** and  $Dat^{ICre/+};R26^{Otx2/Otx2/+};tOtx2^{ov/ov}$  **(i,l)** mutants shows that at late gestation robust Otx2 expression is activated by *Dat*-driven ICre recombinase in virtually all the TH<sup>+</sup> neurons of SNpc and VTA and that the staining due to the activation of Otx2 extra-copies in the SNpc of mutants is comparable in intensity to that of the endogenous Otx2 in the VTA of  $Dat^{ICre/+}$  control mice (compare **h,i** to **j**). Scale bars in **(a,g)** correspond to 100 $\mu$ m **(a)** and 200 $\mu$ m **(g)**; scale bar in **(a)** refers to sections in **(a–f)** and scale bar in **(g)** to sections in **(g–l)**.

**Fig. 2.** Otx2 inactivation does not affect the survival of Otx2<sup>+</sup> VTA neurons but induces an increase in the number of GFP<sup>+</sup>-Girk2<sup>+</sup> neurons. **(a)** Graphic representation showing that, compared to 14-16 week old  $Dat^{ICre/+};Otx2^{GFP/+}$  mice, in  $Dat^{ICre/+};Otx2^{GFP/flox}$  mutants of the same age the post-mitotic inactivation of Otx2 does not affect the internal percentage of GFP<sup>-</sup>-TH<sup>+</sup>, GFP<sup>+</sup>-TH<sup>+</sup> and GFP<sup>+</sup>-TH<sup>-</sup> neurons (\**P* 0.1, \*\**P* 0.18, \*\*\**P* 0.1; *Student t* test). **(b)** Graphic representation showing that in the absence of Otx2, the GFP<sup>+</sup> subpopulation exhibits a selective increase in the percentage of GFP<sup>+</sup>-Girk2<sup>+</sup> neurons (\**P* 0.16; \*\**P* 0.25; \*\*\**P* <<0.001; *Student t* test). **(c–n)** Representative immunohistochemistry experiments on adjacent sections of 14-16 week old  $Dat^{ICre/+};Otx2^{GFP/+}$  and  $Dat^{ICre/+};Otx2^{GFP/flox}$  mice with Otx2-TH **(c,d)**, GFP-TH **(e,f)**, GFP-Calb **(g,h)**, GFP-Ahd2 **(i,j)**, and Girk2-GFP **(k,n)** shows that, compared to control mice, in  $Dat^{ICre/+};Otx2^{GFP/flox}$  mutants Girk2 expression is detected in a

higher number of GFP<sup>+</sup> neurons located in the central VTA (arrows in **m,n**). The dotted lines in (**k–n**) demarcate the central VTA. (**m,n**) Are magnifications of the area boxed in (**k,l**). (D, C and V) in (**k**) stand for presumptive dorsal, central and ventral VTA, respectively. Scale bars in (**c,m**) correspond to 100µm (**c**) and 200 µm (**m**); scale bar in (**c**) refers to sections in (**c–l**) and scale bar in (**m**) to sections in (**m,n**).

**Fig. 3.** Otx2 activation in the VTA generates a reduction in the number of Girk2<sup>+</sup> neurons. (**a**) Graphic representation showing that, compared to 14-16 week old *Dat*<sup>ICre/+</sup> control mice, *Dat*<sup>ICre/+</sup>;*R26*<sup>Otx2/Otx2</sup> and *Dat*<sup>ICre/+</sup>;*R26*<sup>Otx2/Otx2</sup>;*tOtx2*<sup>ov/ov</sup> mutants of the same age exhibit a selective reduction in the percentage of Girk2<sup>+</sup>-TH<sup>+</sup> neurons (\**P* 0.11 and \*\**P* 0.25 for Calb<sup>+</sup>-TH<sup>+</sup> neurons; \**P* 0.2 and \*\**P* 0.24 for Ahd2<sup>+</sup>-TH<sup>+</sup> neurons; and \**P* and \*\**P* <<0.001 for Girk2<sup>+</sup>-TH<sup>+</sup> neurons; *Student t* test). (**b–j**) Representative immunohistochemistry experiments on adjacent sections of *Dat*<sup>ICre/+</sup>, *Dat*<sup>ICre/+</sup>;*R26*<sup>Otx2/Otx2</sup> and *Dat*<sup>ICre/+</sup>;*R26*<sup>Otx2/Otx2</sup>;*tOtx2*<sup>ov/ov</sup> mice with Calb-TH (**b–d**), Ahd2-TH (**e–g**) and Girk2-TH (**h–j**) show that, while no obvious abnormalities are detected for Calb and Ahd2, the number of Girk2<sup>+</sup> neurons and the intensity of their staining is remarkably reduced in Otx2 over-expressing mutants (arrows in **h–j**). Abbreviations as in previous Figure. Scale bar (**b**) refers to all panels and corresponds to 100µm.

**Fig. 4.** The level and the expression profile of glyco-Dat are altered in Otx2 mutants. (**a–d**) Immunohistochemistry experiments on adult wild-type brain with Otx2-glyco-Dat (**a,b**) and Girk2-glyco-Dat (**c,d**) show that the majority of Otx2<sup>+</sup> neurons are glyco-Dat<sup>−</sup> (**a,b**) and that glyco-Dat<sup>+</sup> neurons co-express Girk2 (**c,d**). (**e–h**) Immunohistochemistry experiments on 14-16 week old *Dat*<sup>ICre/+</sup>;*Otx2*<sup>GFP/+</sup> (**e,g**) and *Dat*<sup>ICre/+</sup>;*Otx2*<sup>GFP/flox</sup> (**f,h**) show that in mutants lacking Otx2, the number of GFP<sup>+</sup> neurons co-expressing high level of glyco-Dat is increased

in the central VTA (arrows in **h**). **(i)** Graphic representation showing that, compared to 14-16 week old  $Dat^{ICre/+};Otx2^{GFP/+}$  control mice, in  $Dat^{ICre/+};Otx2^{GFP/lox}$  mutants of the same age, the percentage of GFP<sup>+</sup>-glyco-Dat<sup>+</sup> neurons is significantly increased ( $*P \ll 0.001$ ; *Student t* test). **(j)** Western blot assay showing that the striatal amount of glyco-Dat is diminished in  $Dat^{ICre/+};R26^{Otx2/Otx2};tOtx2^{ov/ov}$  mice. **(k-r)** Immunohistochemistry experiments on 14-16 week old  $Dat^{ICre/+}$  and  $Dat^{ICre/+};R26^{Otx2/Otx2};tOtx2^{ov/ov}$  mice with TH and glyco-Dat show that in the SNpc **(k-n)** and VTA **(o-r)** of mice over-expressing Otx2 the level and the number of glyco-Dat<sup>+</sup> neurons is reduced. **(s)** Graphic representation showing that, compared to  $Dat^{ICre/+}$  control mice, the percentage of TH<sup>+</sup> neurons expressing high level of glyco-Dat is significantly decreased in the SNpc and VTA of  $Dat^{ICre/+};R26^{Otx2/Otx2};tOtx2^{ov/ov}$  mutants ( $*P$  and  $**P \ll 0.001$ ; *Student t* test). Arrows in **(b,g,h)** point to Otx2<sup>+</sup> **(b)** or GFP<sup>+</sup> **(g,h)** neurons expressing high level of glyco-Dat; arrows in **(d)** point to Girk2<sup>+</sup>-glyco-Dat<sup>+</sup> neurons in the central VTA; and arrows in **(q,r)** point to TH<sup>+</sup>-glyco-Dat<sup>+</sup> neurons in the dorsal VTA. Abbreviations as in previous Figures. **(b,d,g,h,m,n,q,r)** Are magnifications of the area boxed in **(a,c,e,f,k,l,o,p)**. Scale bars in **(a,b)** and **(k,m)** correspond to 100 $\mu$ m **(a,b)** and 200 $\mu$ m **(k,m)**. Scale bar in **(a)** refers to sections in **(a,c,e,f,o,p)**; scale bar in **(b)** to sections in **(b,d,g,h,q,r)**; scale bar in **(k)** and **(m)** to sections in **(k,l)** and **(m,n)**, respectively. Full scans of the western blots in **(j)** are presented in **Supplementary Fig. 8**.

**Fig. 5.** Otx2 negatively controls *Dat* mRNA expression. **(a)** Western blot analysis on extracts from ventral pretectum and ventral mesencephalon of 13 week old  $Dat^{ICre/+}$  and  $Dat^{ICre/+};R26^{Otx2/Otx2};tOtx2^{ov/ov}$  mice shows a similar reduction of both glyco-Dat and non-glyco-Dat in mutant mice. **(b)** Semiquantitative RT-PCR assays of *Dat*, *TH* and *Nurr1* in ventral pretectum and ventral mesencephalon show a selective reduction of *Dat* mRNA; RT-PCR assays are performed at 22 (lanes 1 and 3) and 20 (lanes 2 and 4) cycles for *Dat* and

*Nurr1* and at 20 (lanes 1 and 3) and 18 (lanes 2 and 4) cycles for *TH*. (c–n) Glyco-Dat immunohistochemistry (c,d,g,h,k,l) and *Dat* mRNA in situ hybridization (e,f,i,j,m,n) assays on *Dat*<sup>ICre/+</sup>;*Otx2*<sup>GFP/+</sup> (c,e), *Dat*<sup>ICre/+</sup>;*Otx2*<sup>GFP/flox</sup> (d,f), *Dat*<sup>ICre/+</sup> (g,i,k,m) and *Dat*<sup>ICre/+</sup>;*R26*<sup>Otx2/Otx2</sup>;*tOtx2*<sup>ov/ov</sup> (h,j,l,n) mice show that the number of neurons expressing high level of glyco-Dat and *Dat* mRNA is increased in the central VTA of *Dat*<sup>ICre/+</sup>;*Otx2*<sup>GFP/flox</sup> mice (compare c,e to d,f), while, compared to *Dat*<sup>ICre/+</sup> control mice, the number of these neurons is remarkably decreased in both SNpc (g–j) and VTA (k,n) of *Dat*<sup>ICre/+</sup>;*R26*<sup>Otx2/Otx2</sup>;*tOtx2*<sup>ov/ov</sup> mutants. The arrows in (h,j,l,n) point to the residual neurons expressing high level of both glyco-Dat and *Dat* mRNA. Abbreviations as in previous Figures. Scale bars in (c,g) correspond to 100µm (c) and 200µm (g). Scale bar in (c) refers to sections in (c–f, k–n); scale bar in (g) to sections in (g–j). Full scans of the western blots in (a) and RT-PCR assays in (b) are presented in **Supplementary Fig. 8**.

**Fig. 6.** *Otx2* is a neuroprotective factor for the *Otx2*<sup>+</sup> VTA neurons and this property may be conferred to SNpc neurons. (a,b) Graphic representation showing the number of TH<sup>+</sup> neurons and TH<sup>+</sup> subsets expressing GFP (GFP<sup>+</sup>-TH<sup>+</sup>) or silent for GFP (GFP<sup>-</sup>-TH<sup>+</sup>) counted in *Dat*<sup>ICre/+</sup>;*Otx2*<sup>GFP/+</sup> and *Dat*<sup>ICre/+</sup>;*Otx2*<sup>GFP/flox</sup> mice treated with MPTP at 100 mg/Kg (a) and 125 mg/Kg (b), reveals that, compared to control mice, mutants lacking *Otx2* exhibit a significant reduction in the number of total TH<sup>+</sup> and GFP<sup>+</sup>-TH<sup>+</sup> neurons (at 100 mg/Kg of MPTP \**P* < 0.001; \*\**P* 0.005; \*\*\**P* 0.4 and at 125 mg/Kg \**P* and \*\**P* < 0.001; \*\*\**P* 0.3; *Student t* test). (c,d) Graphic representation of the ratio (in %) between MPTP-treated and untreated mice of the same genotype shows that in *Dat*<sup>ICre/+</sup>;*Otx2*<sup>GFP/+</sup> and *Dat*<sup>ICre/+</sup>;*Otx2*<sup>GFP/flox</sup> mice the GFP<sup>-</sup>-TH<sup>+</sup> VTA neuronal subpopulation exhibits a sensitivity to MPTP similar to that detected in the SNpc of *Dat*<sup>ICre/+</sup> (f) or *Dat*<sup>ICre/+</sup>;*Otx2*<sup>GFP/+</sup> (d) control mice; while, compared to *Dat*<sup>ICre/+</sup>;*Otx2*<sup>GFP/+</sup> mice, in *Dat*<sup>ICre/+</sup>;*Otx2*<sup>GFP/flox</sup> mutants the VTA subpopulation of GFP<sup>+</sup>-

TH<sup>+</sup> neurons is more severely affected by MPTP both at 100 mg/Kg (\**P* 0.001; \*\**P* <<0.001; \*\*\**P* 0.1; *Student t* test) (c) and 125 mg/Kg (\**P* and \*\**P* <<0.001; \*\*\**P* 0.4; *Student t* test) (d). (e) Graphic representation showing the number of TH<sup>+</sup> neurons counted in 14-16 week old MPTP-treated *Dat*<sup>ICre/+</sup>, *Dat*<sup>ICre/+;R26<sup>Otx2/Otx2</sup> and *Dat*<sup>ICre/+;R26<sup>Otx2/Otx2</sup>;tOtx2<sup>ov/ov</sup> mice reveals that, compared to *Dat*<sup>ICre/+</sup> mice, mutant mice show a relevant increase in the number of TH<sup>+</sup> neurons in both SNpc and VTA (\**P* and \*\**P* <<0.001 for the SNpc; and \**P* <0.001 and \*\**P* <<0.001 for the VTA; *Student t* test). (f) Graphic representation of the ratio (in %) between MPTP-treated and untreated mice of the same genotype shows that, compared to *Dat*<sup>ICre/+</sup> control mice, SNpc and VTA TH<sup>+</sup> neurons exhibit higher resistance to MPTP in *Dat*<sup>ICre/+;R26<sup>Otx2/Otx2</sup> mice, and are almost insensitive to the neurotoxin in triple mutants (\**P* and \*\**P* <0.001 for the SNpc; \**P* 0.0018 and \*\**P* <<0.001 for the VTA; *Student t* test).</sup></sup></sup>

## METHODS

### Mouse models

The  $R26^{Otx2/+}$  mouse line was generated by targeting in the *Rosa26* locus a plasmid (kindly provided by S. Casola) containing a removable *loxP-Neo* triple polyA-loxP transcriptional stop cassette upstream of a full coding *Otx2 cDNA-Ires GFP* sequence (**Supplementary Fig. 1a**). The linearized construct was electroporated in the E14Tg4a2 ES cell line, and homologous recombination was ascertained by Southern Blot of EcoRI digested genomic DNA (**Supplementary Fig. 1b**) and hybridized with the EcoRI /PacI genomic probe (probe A in **Supplementary Fig. 1a**). To test in vitro the functionality of the transgene and the relative abundance of the inducible  $R26^{Otx2}$  allele, one positive clone was re-transfected to target the CreER recombinase in the second *Rosa26* allele as previously described for the  $tOtx2^{ov}$  allele<sup>6</sup>. One  $R26^{Otx2/CreER}$  clone was selected and tested to quantify the Otx2 and GFP proteins upon removal of the transcriptional block by western blot of crude extracts of ES cells untreated or treated with tamoxifen (**Supplementary Fig. 1c**). The original  $R26^{Otx2/+}$  ES cell clone was injected into C57 blastocysts and chimeras were mated with B6D2 females for germline transmission. Litters were genotyped by PCR with the following primers: forward 5'AAAGTCGCTCTGAGTTGTTATCAG3' and reverse 5'CACACACCAGGTTAGCCTTTAAGC3' for the wild-type allele (254bp long fragment); forward 5'TGATGTATAGTGCCTTGACTAGAG3' and reverse 5'AGGTTGTTTGGAGGCGCGCCGAT3' for the mutant allele (338bp long fragment) (horizontal arrowheads in the first and second line of **Supplementary Fig. 1a**). The  $tOtx2^{ov/+}$ , the  $Dat^{Cre/+}$ , and the  $R26R-LacZ$  mouse strains have been previously described<sup>6,41,50</sup>.

Experiments on animals were performed in accordance with the European Commission guidelines (86/609/CEE) upon approval of Italian Health Ministry, DLgs 116/92.

**Immunohistochemistry and in situ hybridization assays**

Immunohistochemistry and in situ hybridization experiments were performed on PFA fixed, wax-included embryos and brains. The rabbit antibodies were directed against Ahd2 (Abcam, ab24343-200), GFP (Abcam, ab290), Girk2 (Alomone Labs, APC-006), Calb (Swant, CB38), Cre (Novagen, 69050-3), Otx2 (gift of G. Corte), Pitx3 (Zymed Invitrogen, 382850), TH (Chemicon, ab152) and Foxa2 (Abcam, ab40874); the goat antibodies against Ahd2 (Abcam, ab9883), Calb (R&D System, AF3320), Otx2 (R&D System, AF1979), Nurr1 (Santa Cruz Biotechnology, sc900), GFP (Abcam, ab6673) and Pitx3 (N-20) (Santa Cruz Biotechnology, sc19307); the  $\beta$ Gal antibody was raised in chicken (Abcam, ab9361); a second TH antibody was generated in mouse (Chemicon, MAB318); the antibodies against glyco-Dat were raised in rat and corresponded to an IgG2ak (Chemicon, MAB369) and an IgG (Santa Cruz Biotechnology, sc32258) monoclonal antibody, respectively. The in situ probe for *Dat* was a 391 base pairs long RT-PCR fragment.

**RT-PCR and Western blot assays**

Wild-type and mutant adult brains were dissected to isolate approximately the ventral pretecal area and the ventral mesencephalon or the striatum. Tissues were processed to isolate total RNA or protein extracts. Semiquantitative RT-PCR assays were performed in non-saturating conditions for *Dat*, *TH* and *Nurr1*. Primers and detailed procedure are available upon request. For Western blot assays, crude extracts (10  $\mu$ g for striatum and 35  $\mu$ g for pretecal area and mesencephalon) were processed under standard conditions and probed with TH (Chemicon, MAB318) or Dat (Lifespan Biosciences, LS-C11197 or Chemicon, MAB369) antibodies. The Dat antibody from Lifespan Biosciences is an IgG2a monoclonal antibody. Films were processed for densitometric scanning.

### **MPTP treatment**

14-16 or 12-15 week old male mice received a total of 4 or 5 intraperitoneal injections of MPTP (25mg/Kg/injection) at two hours intervals<sup>32</sup> and were sacrificed 7 days after the last injection. Control mice of the same age were injected with saline solution only. The four injections protocol was previously determined and adopted because in our experience, it generates less variability and valuable neuronal loss in the genetic background (C57B6-DBA2) of the mouse strains analyzed. In the five injections protocol approximately 45% of mice died after the last injection.

### **Cell-counting experiments**

Cell-counting experiments were performed on a minimal number of 7 brains and a maximum of 10 brains per genotype (**Supplementary Table 1 and 2**). For wild-type,  $Dat^{ICre/+}$ ,  $Dat^{ICre/+};Otx2^{GFP/+}$ ,  $Dat^{ICre/+};Otx2^{GFP/flox}$ ,  $Dat^{ICre/+};R26^{Otx2/Otx2}$  and  $Dat^{ICre/+};R26^{Otx2/Otx2};tOtx2^{ov/ov}$  mice, we studied male animals at 14-16 or 12-15 weeks of age. For MPTP experiments a total of 20 brains for each genotype were analyzed (10 belong to MPTP-treated and 10 to untreated mice). For TH<sup>+</sup> cell-counting, brains were systematically sectioned in 8 adjacent series of slides and two series (the 3<sup>rd</sup> and the 6<sup>th</sup>) immunostained for TH. Based on the anatomical levels of the SNpc and VTA (**Supplementary Fig. 6**), levels 1 and 6 for both SNpc and VTA were excluded from our analysis and levels 2-5 selected on both sides of the midline and photographed (**Supplementary Fig. 6**). Following this procedure, usually between 8 and 10 images (4-5 sections/brain/emisphere) were selected for the SNpc and VTA, respectively. Pictures were then printed at high magnification in A4 format and TH<sup>+</sup> neurons included in the demarcated areas, were counted (**Supplementary Fig. 6**). For cell-counting of fluorescent immunohistochemistry the same procedure was applied by selecting in this case adjacent series of slides immunostained with different pairs

of antibodies. The total cell numbers, and the mean  $\pm$  the standard deviation (s.d.) were shown (**Supplementary Tables**).

### Statistical analysis

For experiments aimed at defining the numerical size of the different subsets of TH<sup>+</sup> neurons co-expressing in the SNpc and VTA Calb, Ahd2, Girk2 and glyco-Dat, the number of TH<sup>+</sup>-Calb<sup>+</sup>, TH<sup>+</sup>-Ahd2<sup>+</sup>, TH<sup>+</sup>-Girk2<sup>+</sup> and TH<sup>+</sup>-glyco-Dat<sup>+</sup> neurons detected in each brain analyzed were first normalized to the mean of total TH<sup>+</sup> neurons, then, the *P* value was calculated between control and mutants for each marker by using the *one tail Student t* test. The same procedure was applied to *Dat*<sup>ICre/+</sup>;*Otx2*<sup>GFP/+</sup> and *Dat*<sup>ICre/+</sup>;*Otx2*<sup>GFP/flox</sup> mutants to determine both the percentage of TH<sup>+</sup> neurons expressing or not GFP and the fraction of GFP<sup>+</sup> neurons expressing Calb, Ahd2, Girk2 and glyco-Dat. In experiments comparing only the number of TH<sup>+</sup> neurons, the *P* value was determined by collectively comparing the number of TH<sup>+</sup> neurons counted in each brain belonging to a specific genotype to the number of those counted in each brain of the control group. For MPTP experiments aimed at determining TH<sup>+</sup> neuronal loss and corresponding *P* value, TH<sup>+</sup> neurons counted in each of the MPTP-treated brains were collectively compared to those detected in each of the MPTP-untreated brains of the same genotype. A second type of analysis was obtained by collectively comparing TH<sup>+</sup> neurons counted in each of the MPTP-treated mutant brains to those detected in each of the MPTP-treated control brains. For MPTP experiments in *Dat*<sup>ICre/+</sup>;*Otx2*<sup>GFP/+</sup> and *Dat*<sup>ICre/+</sup>;*Otx2*<sup>GFP/flox</sup> mice, the number of TH<sup>+</sup>, GFP<sup>+</sup>-TH<sup>+</sup> and GFP<sup>-</sup>-TH<sup>+</sup> neurons was determined in MPTP-treated and untreated control and mutant mice. GFP<sup>+</sup>-TH<sup>+</sup> and GFP<sup>-</sup>-TH<sup>+</sup> neurons detected in each brain were normalized to the mean of the total number of TH<sup>+</sup> neurons and then, collectively compared between MPTP-treated and untreated mice of the

same genotype; or the same group of neurons (eg. GFP<sup>+</sup>-TH<sup>+</sup>) collectively compared between control and mutants both MPTP-treated.

**REFERENCES**

1. Björklund, A. & Lindvall, O. Dopamine-containing systems in the CNS. In: *Handbook of Chemical Neuroanatomy: Classical Transmitters in the CNS*. Björklund A. and Hökfelt (eds), Elsevier, Amsterdam. **2**, 55-121(1984).
2. Björklund, L. M. & Isacson O. Regulation of dopamine cell type and transmitter function in fetal and stem cell transplantation for Parkinson's disease. *Prog. Brain Res.* **138**, 411-420 (2002).
3. Dahlström, A. & Fuxe, K. Evidence for the existence of monoamine-containing neurons in the central nervous system: I. Demonstration of monoamines in the cell bodies of brain stem neurons. *Acta Physiol. Scand.* **62**, 1-55 (1964).
4. Smidt, M. P. & Burbach, J. P. How to make a mesodiencephalic dopaminergic neuron. *Nat. Rev. Neurosci.* **8**, 21-32 (2007).
5. Marín, F., Herrero, M. T., Vyas, S. & Puellas, L. Ontogeny of tyrosine hydroxylase mRNA expression in mid- and forebrain: neuromeric pattern and novel positive regions. *Dev. Dyn.* **234**, 709-717 (2005).
6. Omodei, D., *et al.* Anterior-posterior graded response to Otx2 controls proliferation and differentiation of dopaminergic progenitors in the ventral mesencephalon. *Development* **135**, 3459-3470 (2008).

7. Thompson, L., Barraud, P., Andersson, E., Kirik, D. & Björklund, A. Identification of dopaminergic neurons of nigral and ventral tegmental area subtypes in grafts of fetal ventral mesencephalon based on cell morphology, protein expression, and efferent projections. *J. Neurosci.* **25**, 6467-6477 (2005).
8. Jellinger, K. A. The pathology of Parkinson's disease. *Adv. Neurol.* **86**, 55-72 (2001).
9. Prakash, N. & Wurst, W. Development of dopaminergic neurons in the mammalian brain. *Cell. Mol. Life. Sci.* **63**, 187-206 (2006).
10. Simeone, A. Genetic control of dopaminergic neuron differentiation. *Trends Neurosci.* **28**, 62-65 (2005).
11. Saucedo-Cardenas, O., *et al.* Nurr1 is essential for the induction of the dopaminergic phenotype and the survival of ventral mesencephalic late dopaminergic precursor neurons. *Proc. Natl. Acad. Sci. USA.* **95**, 4013-4018 (1998).
12. Jankovic, J., Chen, S. & Le, W. D. The role of Nurr1 in the development of dopaminergic neurons and Parkinson's disease. *Prog Neurobiol.* **77**, 128-138 (2005).
13. Smidt, M. P., *et al.* A second independent pathway for development of mesencephalic dopaminergic neurons requires Lmx1b. *Nat. Neurosci.* **3**, 337-341 (2000).
14. Smidt, M. P., *et al.* Early developmental failure of substantia nigra dopamine neurons in mice lacking the homeodomain gene Pitx3. *Development* **131**, 1145-1155 (2004).

15. Kele, J., *et al.* Neurogenin 2 is required for the development of ventral midbrain dopaminergic neurons. *Development* **133**, 495-505 (2006).
16. Ferri, A. L., *et al.* Foxa1 and Foxa2 regulate multiple phases of midbrain dopaminergic neuron development in a dosage-dependent manner. *Development* **134**, 2761-2769 (2007).
17. Andersson, E., Jensen, J. B., Parmar, M., Guillemot, F. & Björklund, A. Development of the mesencephalic dopaminergic neuron system is compromised in the absence of neurogenin 2. *Development* **133**, 507-516 (2006).
18. Andersson, E., *et al.* Identification of intrinsic determinants of midbrain dopamine neurons. *Cell* **124**, 393-405 (2006).
19. Ono, Y., *et al.* Differences in neurogenic potential in floor plate cells along an anteroposterior location: midbrain dopaminergic neurons originate from mesencephalic floor plate cells. *Development*. **134**, 3213-3225 (2007).
20. van den Munckhof, P., *et al.* Pitx3 is required for motor activity and for survival of a subset of midbrain dopaminergic neurons. *Development* **130**, 2535-2542 (2003).
21. Nunes, I., Tovmasian, L. T., Silva, R. M., Burke, R. E. & Goff, S. P. Pitx3 is required for development of substantia nigra dopaminergic neurons. *Proc. Natl. Acad. Sci. USA* **100**, 4245-4250 (2003).

22. Simon, H. H., Saueressig, H., Wurst, W., Goulding, M. D. & O'Leary, D. D. Fate of midbrain dopaminergic neurons controlled by the engrailed genes. *J. Neurosci.* **21**, 3126-3234 (2001).
23. Sonnier, L., *et al.* Progressive loss of dopaminergic neurons in the ventral midbrain of adult mice heterozygote for Engrailed1. *J. Neurosci.* **27**, 1063-1071 (2007).
24. Sgadò, P., *et al.* Slow progressive degeneration of nigral dopaminergic neurons in postnatal Engrailed mutant mice. *Proc. Natl. Acad. Sci. U S A* **103**, 15242-15247 (2006).
25. Zetterström, R. H., *et al.* Dopamine neuron agenesis in Nurr1-deficient mice. *Science* **276**, 248-250 (1997).
26. Castelo-Branco, G., *et al.* Differential regulation of dopaminergic neuron development by Wnt-1, Wnt-3a, and Wnt-5a. *Proc. Natl. Acad. Sci. U S A* **100**, 12747-12752 (2003).
27. Puelles, E., *et al.* Otx dose-dependent integrated control of antero-posterior and dorso-ventral patterning of midbrain. *Nat. Neurosci.* **6**, 453-460 (2003).
28. Puelles, E., *et al.* Otx2 regulates the extent, identity and fate of neuronal progenitor domains in the ventral midbrain. *Development* **131**, 2037-2048 (2004).
29. Prakash, N., *et al.* A Wnt1-regulated genetic network controls the identity and fate of midbrain-dopaminergic progenitors in vivo. *Development* **133**, 89-98 (2006).

30. Afonso-Oramas, D., *et al.* Dopamine transporter glycosylation correlates with the vulnerability of midbrain dopaminergic cells in Parkinson's disease. *Neurobiol. Dis.* **36**, 494-508 (2009).
31. Dauer, W. & Przedborski, S. Parkinson's disease: mechanisms and models. *Neuron* **39**, 889-909 (2003).
32. Jackson-Lewis, V., Jakowec, M., Burke, R. E. & Przedborski, S. Time course and morphology of dopaminergic neuronal death caused by the neurotoxin 1-methyl-4-phenyl-1,2,3,6-tetrahydropyridine. *Neurodegeneration* **4**, 257-269 (1995).
33. Blum, D., *et al.* Molecular pathways involved in the neurotoxicity of 6-OHDA, dopamine and MPTP: contribution to the apoptotic theory in Parkinson's disease. *Prog. Neurobiol.* **65**, 135-172 (2001).
34. Chung, C. Y., *et al.* Cell type-specific gene expression of midbrain dopaminergic neurons reveals molecules involved in their vulnerability and protection. *Hum. Mol. Genet.* **14**, 1709-1725 (2005).
35. Greene, J. G., Dingledine, R. & Greenamyre, J. T. Gene expression profiling of rat midbrain dopamine neurons: implications for selective vulnerability in parkinsonism. *Neurobiol. Dis.* **18**,19-31 (2005).
36. Murer, G., *et al.* An immunocytochemical study on the distribution of two G-protein-gated inward rectifier potassium channels (GIRK2 and GIRK4) in the adult rat brain.

*Neuroscience* **80**, 345-357 (1997).

37. Schein, J. C., Hunter, D. D. & Roffler-Tarlov, S. *Girk2* expression in the ventral midbrain, cerebellum, and olfactory bulb and its relationship to the murine mutation weaver. *Dev. Biol.* **204**, 432-45 (1998).
38. Di Salvio, M., Di Giovannantonio, L. G., Omodei, D., Acampora, D. & Simeone, A. *Otx2* expression is restricted to dopaminergic neurons of the ventral tegmental area in the adult brain. *Int. J. Dev. Biol.* **54**, 939-945 (2010).
39. Liang, C. L., Sinton, C. M., Sonsalla, P. K. & German, D. C. Midbrain dopaminergic neurons in the mouse that contain calbindin-D28k exhibit reduced vulnerability to MPTP-induced neurodegeneration. *Neurodegeneration* **5**, 313-318 (1996).
40. Roffler-Tarlov, S., Martin, B., Graybiel, A. M. & Kauer, J. S. Cell death in the midbrain of the murine mutation weaver. *J. Neurosci.* **16**, 1819-1826 (1996).
41. Bäckman, C. M., *et al.* Characterization of a mouse strain expressing Cre recombinase from the 3' untranslated region of the dopamine transporter locus. *Genesis* **4**, 383-390 (2006).
42. Acampora, D., Di Giovannantonio, L. G., Di Salvio, M., Mancuso, P. & Simeone, A. Selective inactivation of *Otx2* mRNA isoforms reveals isoform-specific requirement for visceral endoderm anteriorization and head morphogenesis and highlights cell diversity in the visceral endoderm. *Mech. Dev.* **126**, 882-897 (2009).

43. Kittappa, R., Chang, W. W., Awatramani, R. B. & McKay, R. D. The *foxa2* gene controls the birth and spontaneous degeneration of dopamine neurons in old age. *PLoS Biol.* **5**, 325 (2007).
44. Li, L. B., *et al.* The role of N-glycosylation in function and surface trafficking of the human dopamine transporter. *J. Biol. Chem.* **279**, 21012-21020 (2004).
45. Torres, G. E., *et al.* Oligomerization and trafficking of the human dopamine transporter. Mutational analysis identifies critical domains important for the functional expression of the transporter. *J. Biol. Chem.* **278**, 2731-2739 (2003).
46. Bezard, E., *et al.* Absence of MPTP-induced neuronal death in mice lacking the dopamine transporter. *Exp. Neurol.* **155**, 268-273 (1999).
47. Pifl, C., Giros, B. & Caron, M. G. Dopamine transporter expression confers cytotoxicity to low doses of the parkinsonism-inducing neurotoxin 1-methyl-4-phenylpyridinium. *J. Neurosci.* **13**, 4246-4253 (1993).
48. Agoston, Z. & Schulte, D. Meis2 competes with the Groucho co-repressor Tle4 for binding to Otx2 and specifies tectal fate without induction of a secondary midbrain-hindbrain boundary organizer. *Development* **136**, 3311-3322 (2009).
49. Kadkhodaei, B., *et al.* Nurr1 is required for maintenance of maturing and adult midbrain dopamine neurons. *J. Neurosci.* **29**, 15923-15932 (2009).

50. Soriano, P. Generalized lacZ expression with the ROSA26 Cre reporter strain. *Nat. Genet.* **21**, 70-71 (1999).

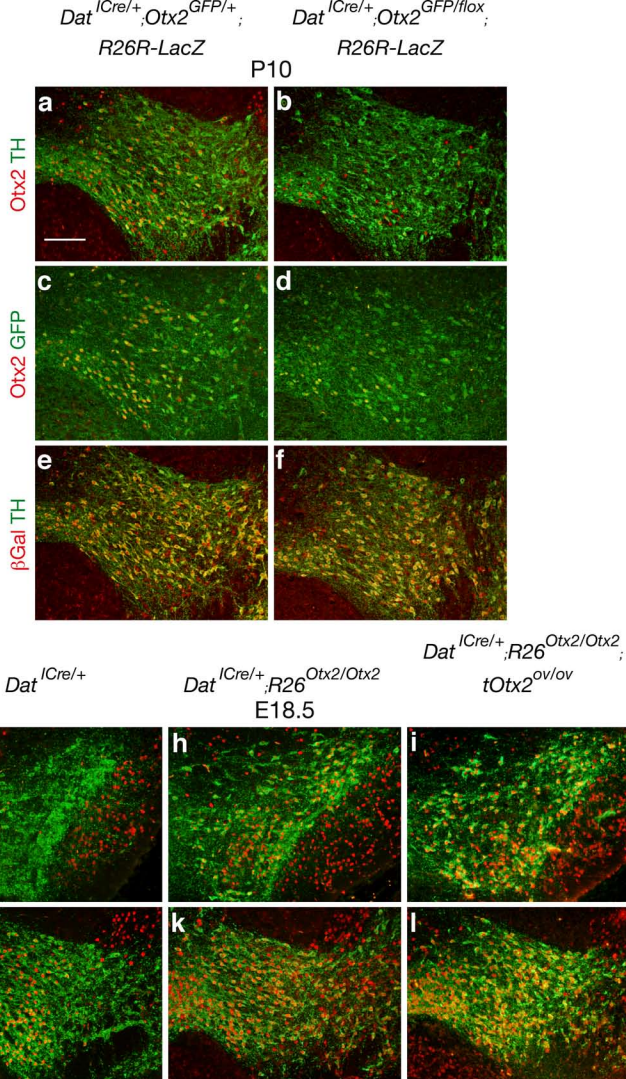


Figure 1 - Di Salvio et al.



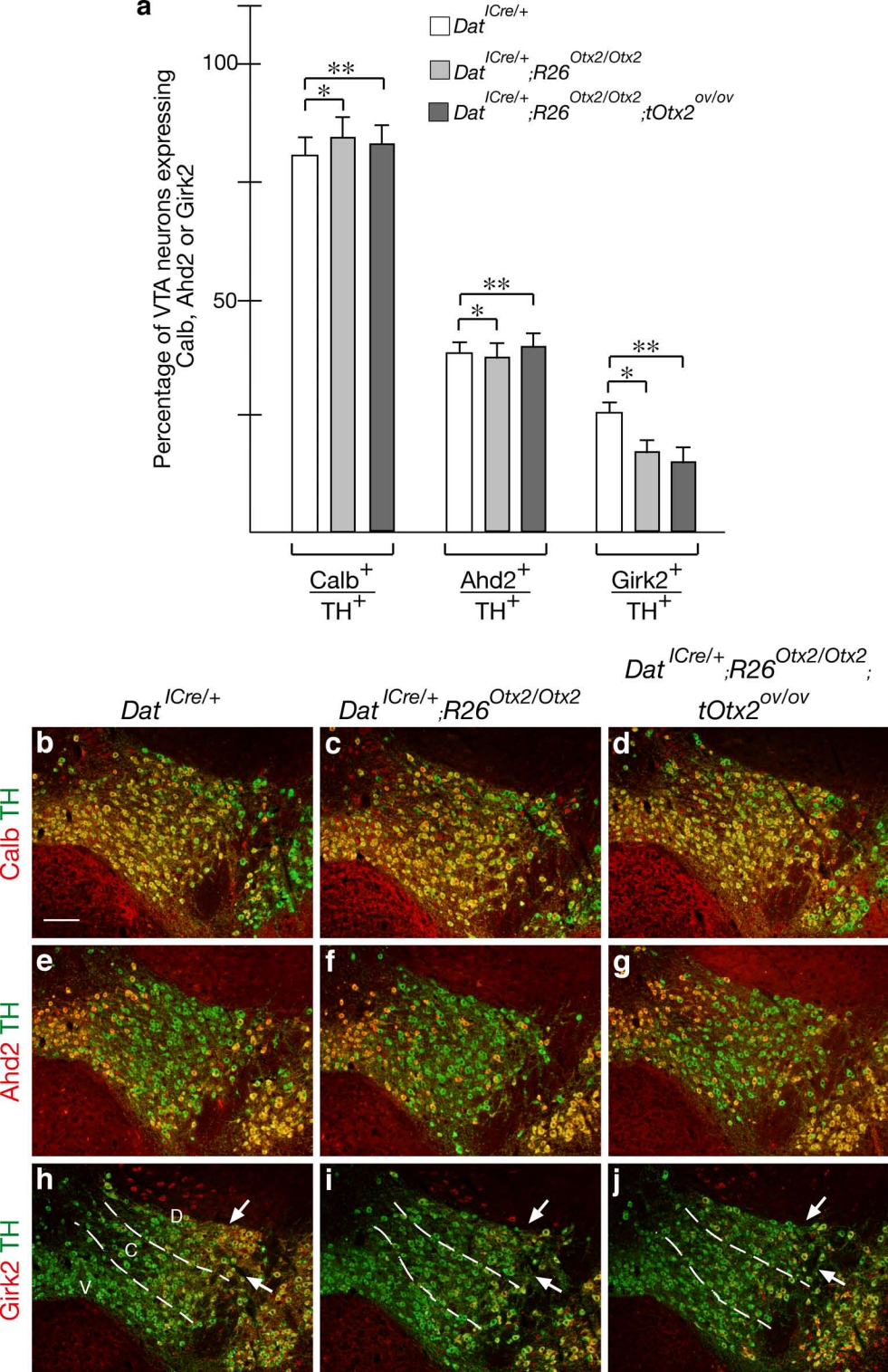


Figure 3 - Di Salvio et al.

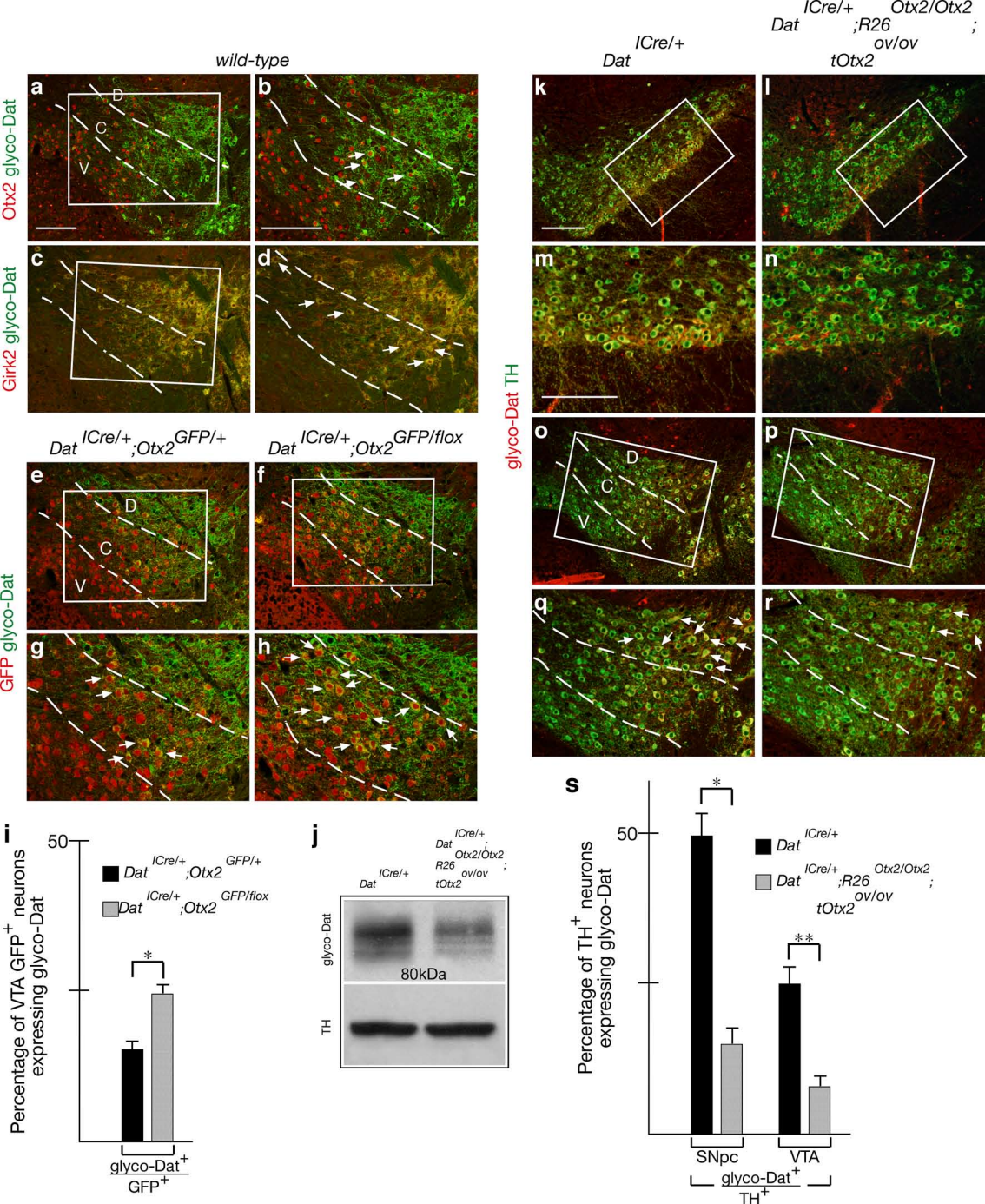


Figure 4 - Di Salvio et al.

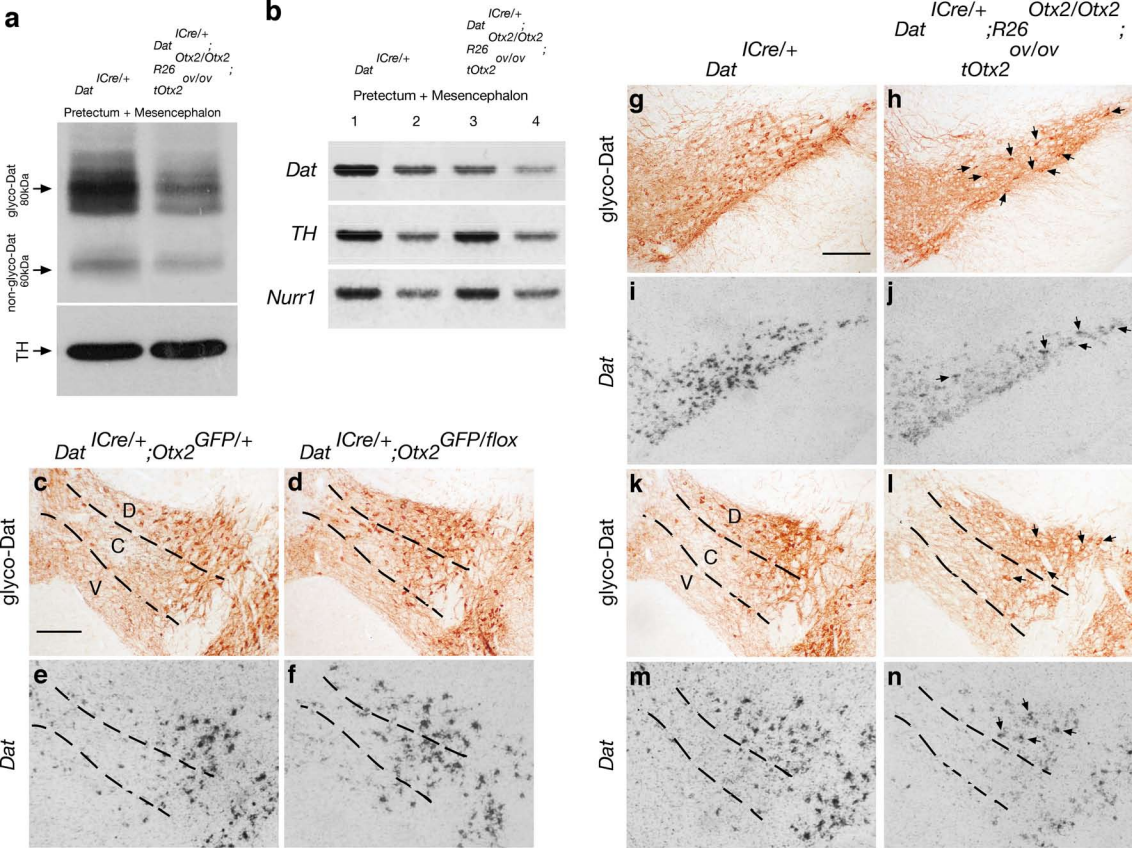


Figure 5 - Di Salvio et al.

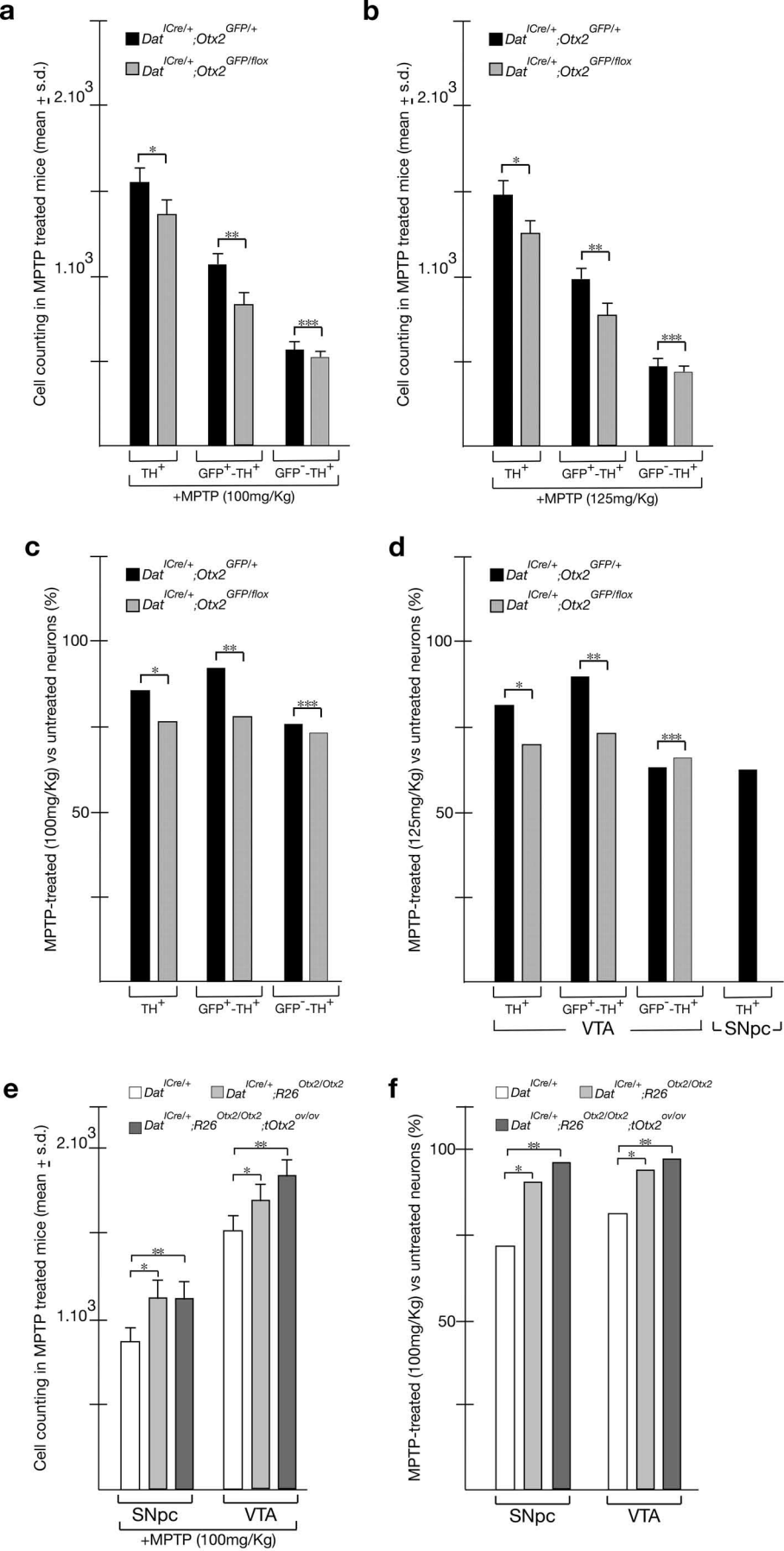


Figure 6 - Di Salvio et al.